

AperTO - Archivio Istituzionale Open Access dell'Università di Torino

The Pyridyl Functional Groups Guide the Formation of Pd Nanoparticles Inside A Porous Poly(4-Vinyl-Pyridine)

This is the author's manuscript

Original Citation:

Availability:

This version is available <http://hdl.handle.net/2318/1531001> since 2015-12-06T21:58:04Z

Published version:

DOI:10.1002/cctc.201500211

Terms of use:

Open Access

Anyone can freely access the full text of works made available as "Open Access". Works made available under a Creative Commons license can be used according to the terms and conditions of said license. Use of all other works requires consent of the right holder (author or publisher) if not exempted from copyright protection by the applicable law.

(Article begins on next page)



UNIVERSITÀ DEGLI STUDI DI TORINO

This is an author version of the contribution published on:

[ChemCatChem 7 (14), pp. 2188-2195 (2015) DOI: 10.1002/cctc.201500211]

The definitive version is available at:

[<http://onlinelibrary.wiley.com/doi/10.1002/cctc.201500211/abstract>]

The pyridyl functional groups guide the formation of palladium nanoparticles inside a porous poly(4-vinyl-pyridine)

Elena Groppo^{*[a]}, Giovanni Agostini^[b], Elisa Borfecchia^[a], Andrea Lazzarini^[a], Wei Liu^[a,+], Carlo Lamberti^[a,c], Francesco Giannici^[d], Giuseppe Portale^[e], and Alessandro Longo^{*[e,f]}

Abstract: The reactivity of palladium acetate inside a poly(4-vinylpyridine-co-divinylbenzene) polymer is strongly influenced by the establishment of interaction between the palladium precursor and the pyridyl functional group in the polymer. DRIFT spectroscopy and simultaneous XANES-SAXS have been applied to monitor the reactivity of palladium acetate in presence of H₂ and CO as a function of temperature. H₂ reduces palladium acetate to palladium nanoparticles and acetic acid. The pyridyl groups in the polymer play a vital role both in stabilizing the formed acetic acid (thus allowing its detection by means of DRIFT) and the final palladium nanoparticles, which are extremely small and mono-dispersed. On the contrary, CO does not reduce palladium acetate. Rather, it forms Pd²⁺-carbonyl adducts, which favor the detachment of the acetate ligands and their thermal degradation. These adducts are well observable by means of SAXS because they cause an important local change of the electronic density.

1. Introduction

It is well known that metal nanoparticles are generally not stable and have the tendency to aggregate in clusters of larger dimension, unless they are supported on solid carriers or suitable stabilizers are added in the synthetic protocol.^[1-3] This is

fundamental to fully exploit the large metal surface area and the enhanced reactivity, which are the most desirable advantages with respect to bulk materials of identical composition and one of the vital property for most of the applications in nano-technology. Polymers may act simultaneously as supports and as stabilizers for metal nanoparticles, and the resultant supported metals usually display unique physical-chemical properties.^[4-12] The stabilizing effect of a polymer towards metal nanoparticles depends on both the available surface area (steric stabilization) and the chemical composition (electrostatic stabilization). In particular, for polymers not containing specific functional groups (such as polystyrene-based polymers), stabilization may occur only through a simple electronic interaction (e.g. between the π -electrons of the benzene rings of the polystyrene-based polymer and the vacant orbitals of metal atoms).^[9,13] On the contrary, when polymers characterized by specific functional groups are used, an additional stabilization mechanism, involving a σ -type coordination between the heterodonor atoms present in the functional groups and the surface of the metal nanoparticles, may take place. It is worth of note that similar effect happens in solution in presence of classical stabilizers, such as carboxylic acids, thiols, or amines.^[14] Porous polymers having functional groups are very interesting in this respect, because they allow to tune the properties of the supported nanoparticles by acting simultaneously on the two stabilization mechanisms (steric and electrostatic).

The use of polymers as supports for metal nanoparticles is particularly attractive in the field of catalysis.^[15-20] For example, polymer-supported palladium-based catalysts have shown remarkable performance in coupling and hydrogenation reactions.^[21] In this contest, we have been recently involved in a thorough investigation on palladium-based catalysts supported on highly cross-linked polymers characterized by a permanent porosity. In a previous work of this series, we demonstrated that these polymers (namely, a poly(ethylstyrene-co-divinylbenzene) and a poly(4-vinylpyridine-co-divinylbenzene), both of them having commercial origin) efficiently stabilize palladium nanoparticles, whose final properties depend on the chemical composition of the polymer matrix.^[22] In particular, it was found that the nitrogen-based ligands in the poly(4-vinylpyridine-co-divinylbenzene) (hereafter P4VP) polymer stabilize extremely small palladium nanoparticles having a very homogeneous dispersion (average particle size of 1.5 nm with a standard deviation of 0.3 nm as evaluated by a systematic HR-TEM analysis on a statistically significant number of particles, and even smaller dimension as estimated by EXAFS data analysis). More recently, we monitored *in situ* the formation of palladium nanoparticles inside the poly(ethylstyrene-co-divinylbenzene) polymer (i.e. without functional groups).^[23] We proved that the reduction process of palladium acetate inside the polymer and the concomitant formation of Pd nanoparticles can be efficiently

[a] Dr. E. Groppo, Dr. E. Borfecchia, A. Lazzarini, Dr. W. Liu, Prof. Dr. C. Lamberti
Department of Chemistry, INSTM and NIS Centre
University of Torino
via Quarello 15, I-10135 Torino (Italy)
E-mail: elena.groppo@unito.it

[b] Dr. G. Agostini
European Synchrotron Radiation Facility,
6 Rue Jules Horowitz, 38043 Grenoble, France

[c] Prof. Dr. C. Lamberti
Southern Federal University
Zorge Street 5, 344090 Rostov-on-Don, Russia

[d] Dr. F. Giannici
Dipartimento di Fisica e Chimica
Università di Palermo
Viale delle Scienze, I-90128 Palermo, Italy

[e] Dr. G. Portale, Dr. A. Longo
Netherlands Organization for Scientific Research at ESRF
BP 220, F-38043 Grenoble Cedex 9, France

[f] Dr. A. Longo
Consiglio Nazionale delle Ricerche, Istituto per lo Studio dei
Materiali Nanostrutturati, Sezione di Palermo
Via La Malfa, 153, I-90146 Palermo, Italy
E-mail: alessandro.longo@esrf.fr

[+] Dr. Liu Wei
Current address: State Key Laboratory of Hollow-fiber Membrane
Materials and Membrane Processes, School of Environmental and
Chemical Engineering
Tianjin Polytechnic University, Tianjin 300387, People's Republic of
China

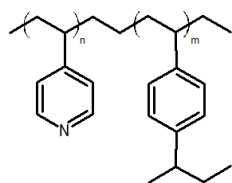
monitored by simultaneously applying SAXS and XANES techniques in reaction conditions, coupled with other techniques such as DRIFT spectroscopy.

Herein, we apply the same methodology to monitor the formation of palladium nanoparticles (starting from palladium acetate precursor) inside the P4VP matrix (i.e. in presence of nitrogen-containing functional groups) in presence of H_2 . These data, collected in operando, complement those reported in our previous publication (collected on ex-situ treated samples)^[22] and add interesting information on the mechanism of palladium acetate reduction and palladium nanoparticles formation. In addition, the reactivity of the same system towards CO is also investigated for the first time. Indeed, in certain reaction conditions CO is known to reduce Pd(II) compounds to give palladium nanoparticles exhibiting unusual shapes,^[7,24] likely due to the fact that CO stabilizes certain faces with respect to others. A comparison of the results with those obtained previously for palladium acetate in poly(ethylstyrene-co-divinylbenzene)^[23] will allow us to elucidate the role of the pyridyl functional groups on the palladium nanoparticle formation.

2. Results and Discussion

2.1. The P4VP/Pd(OAc)₂ system

The P4VP/Pd(OAc)₂ starting material was obtained upon impregnating a commercial P4VP polymer (Scheme 1) with a solution of palladium acetate in acetonitrile, resulting into a final Pd loading of 5 wt%. Details on the synthesis procedure and on the polymer are given in the Experimental section.



Scheme 1. A sketch of the P4VP polymer.

DRIFT spectroscopy was used to obtain preliminary information on the structure of palladium acetate inside the P4VP scaffold. Figure 1 shows the DRIFT spectra of the P4VP/Pd(OAc)₂ system (spectrum 2) compared to that of P4VP (spectrum 1). The first observation is that some IR absorption bands characteristic of the pyridyl group in the polymer are shifted after insertion of palladium acetate. In particular, the two bands at 1596 and 1414 cm^{-1} , which are assigned to the 8a and 19b vibrational modes of pyridyl functional group,^[25] shift at 1640 and 1430 cm^{-1} , respectively (arrows in Figure 1). Similar shifts of the IR absorption bands typical of the pyridyl groups in P4VP were reported for several P4VP/metal complexes,^[26-32] testifying the occurrence of a strong interaction between the pyridyl groups of the polymer and the hosted metal precursors. Hence, insertion of palladium acetate into the P4VP scaffold occurs

through chemical interactions involving the pyridyl groups in the polymer.

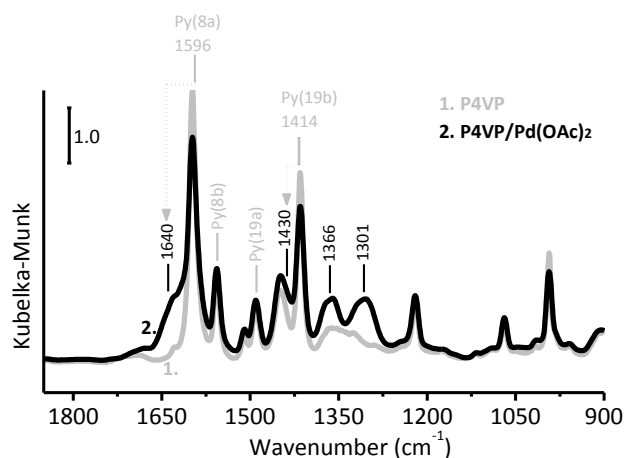
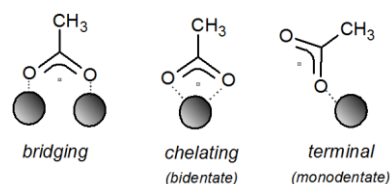


Figure 1. DRIFT spectrum (in Kubelka-Munk units) of P4VP/Pd(OAc)₂ (spectrum 2) compared to that of pure P4VP (spectrum 1); both samples were degassed at room temperature. The spectra are shown in the 1850–900 cm^{-1} region, where the most intense IR absorption bands characteristic of both the vinyl pyridyl functional groups (belonging to P4VP) and the acetate moieties (belonging to Pd(OAc)₂) are observed. The absorption bands relevant for the discussion are also assigned.

In addition, two broad IR absorption bands centered at 1366 and 1301 cm^{-1} are observed in the spectrum of P4VP/Pd(OAc)₂, which are due to the $\nu(COO)$ vibrational modes of the acetate groups. The frequency position of these bands is much lower than for solid palladium acetate and reflects a different local structure of the acetate.^[33-35] For a series of acetate complexes, it has been shown that $\nu_{asym}(COO)$ and $\nu_{sym}(COO)$ change as a function of the acetate coordination mode (bridging, chelating or terminal in Scheme 2).^[36] In particular, $\nu_{asym}(COO)$ increases and $\nu_{sym}(COO)$ decreases as the metal-O bond became stronger.^[36] Indeed, when the metal-to-oxygen bonds are strong, the $\nu_{asym}(COO)$ vibration is more properly described as a C=O stretch, whereas the $\nu_{sym}(COO)$ approximates a C-O motion with little contributions from the rest of the molecule. Correspondingly, the frequency separation between these two modes is larger for terminal (monodentate) acetates than for bridging and chelating (bidentate) acetates.^[33-35]



Scheme 2. Possible coordination modes for an acetate ligand to a metal site (grey ball).

In agreement with this general trend, the $\nu_{\text{asym}}(\text{COO})$ and $\nu_{\text{sym}}(\text{COO})$ frequency values for palladium acetates are around 1615 and 1430 cm^{-1} for trimers (where both bridging and chelating acetates are present),^[37] and 1630 and 1315 cm^{-1} for terminal acetates (mono-dentate),^[34] respectively. On these basis, the couple of bands at 1366 and 1301 cm^{-1} in the spectrum of P4VP/Pd(OAc)₂ are tentatively assigned to the $\nu_{\text{sym}}(\text{COO})$ modes of two slightly different terminal acetate ligands, being the $\nu_{\text{asym}}(\text{COO})$ mode mixed with the absorption band previously assigned to the perturbed 8a mode of the pyridyl groups (around 1630 cm^{-1}). Hence, the DRIFT spectra shown in Figure 1 suggest that when palladium acetate is inserted into P4VP the acetate ligands have mainly a mono-dentate coordination. In conclusion, DRIFT spectroscopy reveals that palladium acetate is stabilized inside the P4VP scaffold through the coordination of the pyridyl groups to the Pd²⁺ cations, with the consequent rupture of the trimeric structure characteristic for solid palladium acetate, and the restructuring of the acetate ligands in a mono-dentate coordination.

2.2. Reduction of P4VP/Pd(OAc)₂ in presence of H₂: formation of Pd nanoparticles in P4VP

DRIFT spectroscopy was successively employed to monitor in situ the reduction of P4VP/Pd(OAc)₂ in presence of gaseous H₂ as a function of temperature. The sequence of DRIFT spectra collected during the reaction is shown in Figure 2: part a) shows the spectra collected from room temperature to 110 °C, while part b) shows the spectra collected in the 110-200 °C interval.

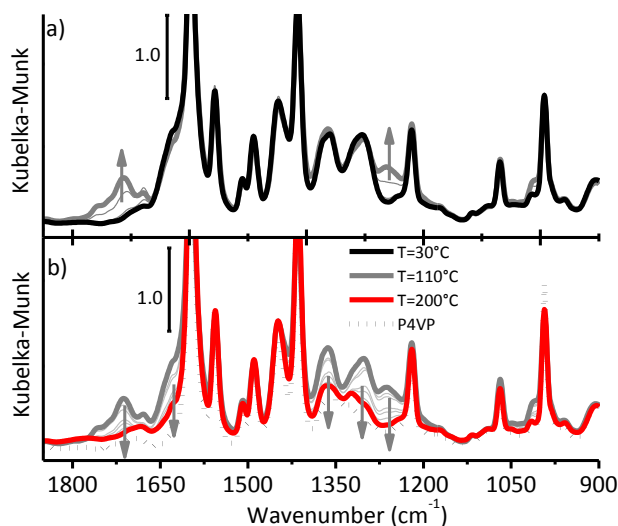


Figure 2. DRIFT spectra (in Kubelka-Munk units) collected during reduction of P4VP/Pd(OAc)₂ in H₂ from room temperature (black) to 200 °C (red), heating rate 2 °C/min. Part a) refers to the first part of the heating ramp (room temperature – 110 °C), and highlights the formation of acetic acid (grey arrows). Part b) shows the evolution of the spectra during the successive part of the heating ramp (110 °C to 200 °C): acetic acid is removed and the absorption bands due to acetate ligands decrease in intensity (grey arrows). Also the spectrum of pure polymer is shown for comparison (dotted black).

Below 110 °C only minor modifications are observed in the spectrum of P4VP/Pd(OAc)₂, except for the appearance of additional IR absorption bands around 1715 and 1260 cm^{-1} (see arrows), which are easily ascribed to acetic acid.^[36] Above 110 °C these bands gradually disappear, accompanied by the decrease in intensity of the IR absorption bands characteristic of the acetate groups (see arrows). The spectrum collected at 200 °C is very similar to that of bare P4VP. This observation provides evidence that the pyridyl functional groups in P4VP are no more in interaction with Pd²⁺ cations and that the acetate ligands have been completely removed. The decrease in intensity of the IR absorption band at 1365 cm^{-1} (characteristic of acetate ligands) as a function of temperature gives a rough estimation of the reaction kinetics (vide infra Figure 4a).

According to DRIFT data, reduction of palladium acetate in P4VP proceeds through the formation of acetic acid. The presence of the basic pyridyl groups in the polymer matrix allows the spectroscopic observation of acetic acid, which is likely coordinated to pyridyl groups up to around 110 °C. Above 110 °C, acetic acid is desorbed, and the equilibrium of the reaction is rapidly shifted towards the products side. It is interesting to observe that when the same reaction is monitored for palladium acetate in the poly(4-ethylstyrene-co-divinylbenzene) matrix, which has no functional groups, acetic acid is not detected by DRIFT.^[23] The sample at the end of the DRIFT experiment was investigated by HR-TEM. A representative image is shown in Figure 3. Very small Pd nanoparticles with a spherical shape and a very narrow size distribution are homogeneously distributed in the polymer matrix: most of them have a diameter smaller than 2 nm, in good agreement with our previous data.^[22]

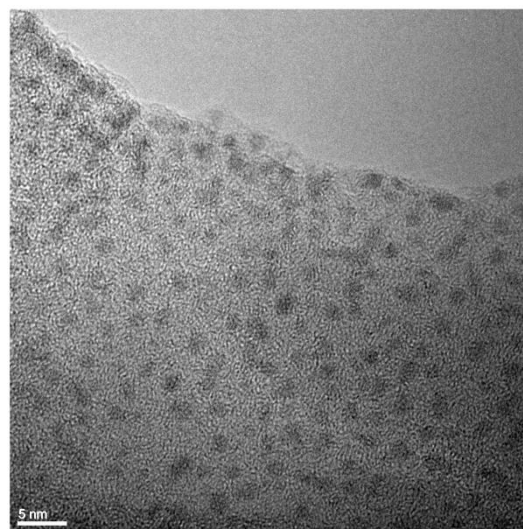


Figure 3. Representative HR-TEM image of the Pd particles obtained upon reduction of P4VP/Pd(OAc)₂ in H₂ during the DRIFT experiment shown in Figure 2.

Successively, the same reaction was followed by means of simultaneous SAXS and XAS techniques, in order to get

combined information from the Pd perspective. As demonstrated in the previous work of this series,^[23] SAXS and XAS applied simultaneously in reaction conditions may provide information on the evolution of the Pd oxidation state, the size of the formed Pd nanoparticles or aggregates, and the quantity of Pd contributing to the total scattering as a function of both time and temperature.^[38-44] Figure 4 shows the evolution of the normalized XANES spectra and SAXS patterns (in log-log scale) at the Pd K-edge, collected simultaneously during thermal treatment of P4VP/Pd(OAc)₂ in gaseous H₂ from room temperature (black) to 200 °C (red). The experimental details are given in the Experimental section.

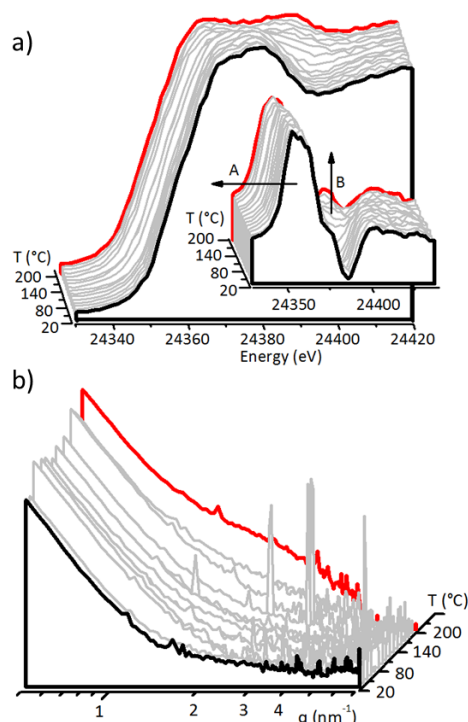


Figure 4. Evolution of the normalized Pd K-edge XAS spectra (part a) and SAXS patterns (in log-log scale, part b) collected simultaneously during reduction of P4VP/Pd(OAc)₂ in H₂ from room temperature (black) to 200 °C (red); heating rate 2 °C/min. The inset in part a) shows the derivative of the normalized XANES spectra.

During the reaction, the XANES spectra (Figure 4a) gradually evolve, testifying a progressive reduction of the Pd²⁺ precursor and the formation of Pd⁰ nanoparticles. In particular, the edge shifts to lower energy, and a weak band slowly grows at 24393 eV, which is assigned to the first EXAFS oscillation of palladium atoms arranged in a fcc local structure.^[22,23] The evolution of the spectra is better appreciated by looking at their derivative (inset in Figure 5a). The energy position of feature A and the intensity of feature B are shown as a function of temperature in Figure 5b. The energy position of feature A (ΔE_A) correlates with the edge position, and hence gives information on the oxidation state of palladium. It is evident that almost no

reduction occurs up to about 110 °C, in fair agreement with the DRIFT data (Figure 5a). The growth in intensity of feature B in the derivative of the XANES spectra (ΔI_B) correlates, in a first approximation, with the dimension of the formed Pd⁰ nanoparticles. Feature B grows in intensity as soon as feature A starts to change. The final intensity of feature B (0.02 eV⁻¹) is much smaller than that observed in the spectrum of a palladium metal foil (0.04 eV⁻¹),^[22] as expected in case of very small nanoparticles, due to the significant fraction of low-coordination surface sites over the total number of Pd-metal sites.

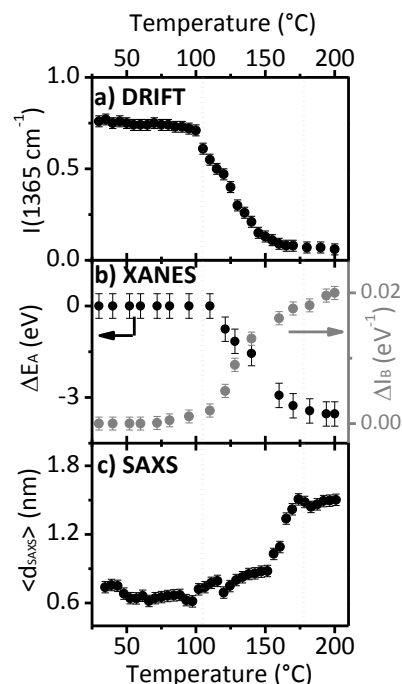


Figure 5. Evolution as a function of temperature and in presence of H₂ of: part a) the intensity of the IR absorption band at 1365 cm⁻¹, which is characteristic of the acetate ligands; part b) features A (shift in energy) and B (change in intensity) of the derivative XANES spectra (see arrows in the inset of Figure 4a); part c) average Pd particle size as obtained from analysis of the SAXS data shown in Figure 4b.

Complementary information on the Pd particle size can be obtained by the analysis of the SAXS data collected simultaneously to the XANES spectra. Figure 5b shows the evolution as a function of temperature of the $I(q)$ vs the module of scattering vector q in the logarithmic scale for P4VP/Pd(OAc)₂ during the heating ramp in gaseous H₂. The patterns start to change for temperatures above 110 °C, in agreement with the previously discussed results. The SAXS data have been analyzed by fitting the experimental patterns according to calculated function described by equation (1):

$$I(q) = A + \frac{B}{q^4} + C \int D(r) j(qR)^2 r^6 dr \quad (1)$$

Where: the function $A + B/q^4$ is the Porod function simulating the polymer contribution; $D(r)$ is the Weibull function accounting for the particle size distribution, defined as $D(r) = (r/R)^{b-1} \exp(-r/R)^b$

where R is the mean radius of the particles; and $j(qR)$ is the Bessel function of order 1 accounting for spherical shape of the metal clusters. Figure 5c shows the evolution of the average particle diameter. Below about 110 °C the particle diameter ($\langle d_{\text{SAXS}} \rangle = 2R$) remains almost constant around 0.7 ± 0.05 nm; when reduction of palladium acetate begins, the average particle diameter increases up to reach a final value around 1.5 ± 0.05 nm, which is in good agreement with the value estimated by HR-TEM; measurements (Figure 3) and with that reported previously for a similar P4VP/Pd(OAc)₂ sample reduced in H₂ in static conditions.^[22]

The data summarized in Figure 5 can be directly compared with those obtained for palladium acetate inside the poly(ethylstyrene-co-divinylbenzene) (i.e. in absence of functional groups in the matrix).^[23] The presence of nitrogen-containing functional groups is responsible, at first, of a greater stabilization of palladium acetate and the simultaneous stabilization of acetic acid, which is the by-product in the H₂-reduction process; the consequence is that palladium acetate is reduced at higher temperature in P4VP than in poly(ethylstyrene-co-divinylbenzene). Moreover, much smaller palladium nanoparticles are formed in P4VP.

2.3 Inefficiency of CO in reducing the P4VP/Pd(OAc)₂ system

In a second moment, we investigated the reactivity of the P4VP/Pd(OAc)₂ system in presence of carbon monoxide.

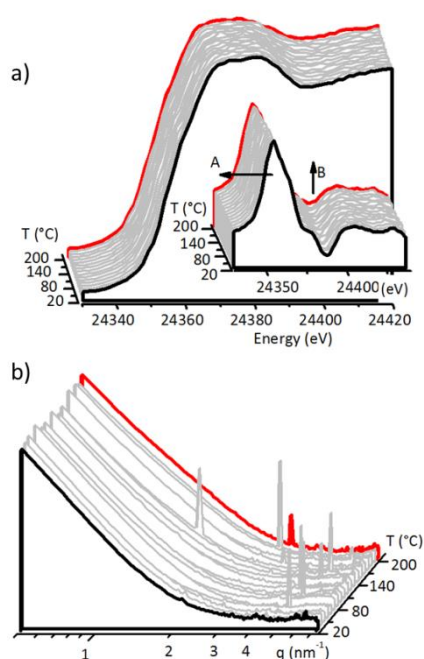


Figure 6. Evolution of the normalized Pd K-edge XAS spectra (part a) and SAXS patterns (in log-log scale, part b) collected simultaneously during reaction of P4VP/Pd(OAc)₂ in CO from room temperature (black) to 200 °C (red); heating rate 2 °C/min. The inset in part a) shows the derivative of the normalized XANES spectra.

CO was found to be an efficient reducing agent for palladium acetate in poly(ethylstyrene-co-divinylbenzene), where it causes the formation of bigger palladium nanoparticles characterized by a triangular morphology.^[23] Surprisingly, we found that CO does not reduce palladium acetate at all in P4VP, as already evident by looking to the color of the sample (that remains pale yellow).

Figure 6 shows the evolution of the XANES spectra and SAXS patterns at the Pd K-edge, collected simultaneously during thermal treatment of P4VP/Pd(OAc)₂ in gaseous CO from room temperature (black) to 200 °C (red). It is evident that the XANES spectra remain almost the same along the whole reaction, providing evidence that the Pd²⁺ cations are reduced by CO only in minimal part. The evolution as a function of temperature of features A and B in the derivative of the XANES spectra is shown in Figure 7b. On the contrary, SAXS patterns starts to change immediately after the beginning of the reaction. This change cannot be ascribed to the formation of palladium nanoparticles, since the XANES spectra collected simultaneously do not reveal any reduction phenomenon. Figure 7c reports the evolution as a function of temperature of the average diameter of aggregates characterized by a different electronic density with respect to the starting palladium acetate precursor.

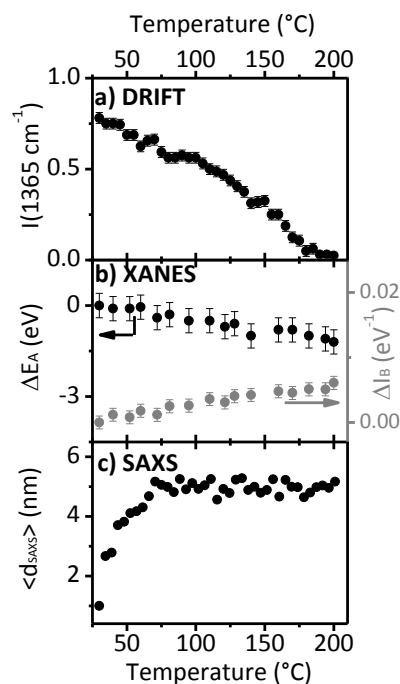


Figure 7. Evolution as a function of temperature in presence of CO of: part a) the intensity of the IR absorption band at 1365 cm⁻¹, which is characteristic of the acetate ligands; part b) features A (shift in energy) and B (change in intensity) of the derivative XANES spectra (see arrows in the inset of Figure 6a); part c) average particle size as obtained from analysis of the SAXS data shown in Figure 6b.

DRIFT spectroscopy may help in understanding the origin of this interesting observation, i.e. a great change in the SAXS

pattern which is not by significant modifications in the XANES spectra. The whole series of DRIFT spectra collected during reaction of P4VP/Pd(OAc)₂ in presence of CO as a function of temperature is shown in Figure 8; part a) shows the spectra collected from room temperature to 110 °C, and part b) those collected in the 110 – 200 °C interval. The first observation to be done is the rapid appearance in the DRIFT spectra of a broad band at 2170 cm⁻¹ (inset in Figure 8a), overlapped to the rotovibrational profile of gaseous CO. This band may be assigned to the formation of Pd²⁺ carbonyls. Similar high $\nu(\text{CO})$ values have been reported for highly electrophilic CO complexes of Pt and Pd, characterized by a negligible metal-CO π -back bonding and an enhanced π -acceptor ability of the ligand, and also for isolated Pd²⁺ carbonyls formed in zeolites.^[45,46] Simultaneously, the IR absorption bands characteristic of mono-dentate acetate ligands shift downward from 1372 to 1360 cm⁻¹ and from 1320 to 1300 cm⁻¹, probably as a consequence of a further change in the geometry of the acetate ligands induced by the insertion of CO into the Pd²⁺ coordination sphere. Finally, the IR absorption bands characteristic of the acetate groups start to decrease in intensity since the beginning of the reaction, opposite to what observed in presence of H₂. At temperature above 110 °C these bands gradually disappear. Nevertheless, the disappearance of the acetate ligands should be ascribed to their thermal degradation and not to the reduction of palladium acetate, according to the XANES results.

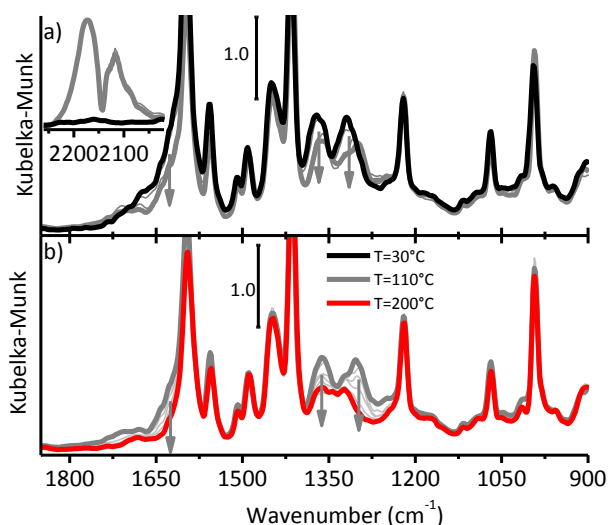


Figure 8. DRIFT spectra (in Kubelka-Munk units) collected during reduction of P4VP/Pd(OAc)₂ in CO from room temperature (black) to 200 °C (red), heating rate 2 °C/min. Part a) refers to the first part of the heating ramp (room temperature – 110 °C). Grey arrows highlight the decrease of the IR absorption bands due to the acetate ligands. The inset shows the $\nu(\text{CO})$ spectral region. Part b) shows the evolution of the spectra during the successive part of the heating ramp (110 °C - 200 °C): the absorption bands due to acetate ligands further decrease in intensity (grey arrows).

In summary, CO seems not able to reduce the palladium acetate stabilized in P4VP. Likely, isolated Pd²⁺ carbonyls are

immediately formed, with the concomitant displacement of the acetate ligands. The so formed Pd²⁺ carbonyls are no longer bond to the nitrogen atoms of the pyridyl units of the polymer matrix as it was the case for the palladium acetate precursor and they can migrate and aggregate. The aggregation of Pd²⁺ carbonyls causes a net local change of the electronic density in the polymer matrix, with the consequent rapid change of the SAXS patterns. These carbonyls are not able to further evolve into metal nanoparticles.

3. Conclusions

The combined use of DRIFT spectroscopy and simultaneous XANES-SAXS allowed us to monitor the reactivity of palladium acetate in a P4VP polymer towards different reducing agents as a function of temperature and to get insights into the important roles played by functional groups in polymeric matrices during the formation of palladium nanoparticles.

We have demonstrated that the presence of pyridyl functional groups inside P4VP facilitates the dispersion of palladium acetate in a monomeric form, in which the acetate ligands assume a mono-dentate configuration. This peculiar structure of palladium acetate in P4VP is at the basis of its different reactivity towards reducing agents with respect to what observed for palladium acetate inside a similar polymer without functional groups. It was demonstrated that H₂ efficiently reduces palladium acetate in P4VP, to give palladium nanoparticles and acetic acid. The latter is stabilized by the basic functional groups in the polymer, which make possible its spectroscopic observation. The consequence is that reduction occurs at a higher temperature than for palladium acetate dispersed in a similar polymer without functional groups, as determined by DRIFT and XANES spectroscopy.^[23] In addition, the palladium nanoparticles are also smaller (as determined by SAXS), because stabilized by direct covalent interaction with the nitrogen-containing ligands, in fair agreement with previous findings.^[22] On the contrary, CO does not reduce palladium acetate. Isolated Pd²⁺ carbonyl adducts are immediately formed, with the simultaneous displacement of the acetate ligands, as detected by DRIFT spectroscopy. These Pd²⁺ carbonyl adducts easily migrate and aggregate in units of about 5 nm that, having a higher electronic density with respect to the polymer matrix, are clearly revealed by SAXS.

The results discussed in this work demonstrate that the establishment of interaction between a metal precursor and the polymer matrix plays a fundamental role in determining the reactivity of the metal precursor. Chemical reactions in confined spaces where strong interactions may take place are completely different from those occurring in non-confined spaces. These findings have important potential implications in the field of catalysis. For example, it is expected that reactions catalyzed by palladium acetate and involving carbon monoxide would have a different outcome when palladium acetate is hosted in porous P4VP than in other supports without pores and/or nitrogen containing ligands. As a general conclusion, this work demonstrates the role of combined synchrotron radiation

techniques in the characterization of nanostructured materials.^[47-50]

4. Experimental Section

The polymer used as a matrix for palladium acetate is a poly(divinylbenzene-co-4-vinylpyridine) (P4VP in the text), showing a specific surface area of about 50 m²g⁻¹. The polymer was impregnated with a solution of palladium acetate in acetonitrile, resulting in a final palladium loading of 5 wt%. After impregnation, the sample was filtered and dried at room temperature. The so obtained P4VP/Pd(OAc)₂ sample was successively heated in gas flow, either CO(5%)/He or H₂(5%)/He at 25 ml/min. During each treatment, the temperature of the sample (in the powder form) was raised from 25 °C to 200 °C, at a heating rate of 2 °C/min. The process was monitored in situ either by DRIFT or by means of simultaneously applied XANES and SAXS techniques.

FT-IR spectra were collected in reflectance mode (DRIFT) on a Nicolet6700 instrument, equipped with a MCT detector. A Thermo Fisher Environmental Chamber was adopted to record FT-IR spectra in reaction conditions. FT-IR spectra were recorded at regular time interval during the whole process at a spectral resolution of 4 cm⁻¹.

In situ XAS and SAXS measurements were carried out simultaneously on the BM26A beamline at the ESRF facility (Grenoble, France), using the experimental set-up previously reported.^[51,52] The powdered samples were placed in a 2 mm glass capillary connected to gas flow, and heated with a heat gun. Fluorescence XAS spectra at the Pd K-edge (24.35 keV) were collected with a 9-element Ge detector. The energy delivered by the double crystal Si(111) monochromator was calibrated measuring the XANES spectrum of a palladium foil in transmission mode. The spectra were normalized and treated with the Athena software.^[53] The SAXS patterns were collected using a 2D Mar CCD detector. The sample-detector distance was calibrated accordingly to the peak position of a standard Ag behenate powder sample. The energy change between the start and the end of the XAS spectrum (about 120 eV) is irrelevant to SAXS collected with a so high photon energy, so that the incident beam wavelength can be treated as constant, $\lambda = 0.509(1)$ Å. The resulting q -range was 0.5 – 7 nm⁻¹ (with the module of the scattering vector $q = 4\pi\sin\theta/\lambda$, where θ is half of the scattering angle), allowing to investigate the 12.5–0.7 nm d -spacing interval (being $d = 2\pi/q$). Each XAS spectrum was collected in about 300 s. As the readout and erasing time of the 2D Mar detector was of 180 s, each XAS spectrum was collected with an integration statistics of 120 s; in such a way we obtained a 1 to 1 correspondence between XAS spectra and SAXS patterns. The patterns were integrated with Fit2D and modeled using a home-made code.^[54]

Acknowledgements

Riccardo Pellegrini and Adriano Zecchina are kindly acknowledged for useful discussion. C. L. acknowledges the Mega-grant of the Russian Federation Government to support scientific research under the at Southern Federal University, No. 14.Y26.31.0001.

Keywords: palladium • X-ray absorption spectroscopy • Small-angle X-ray spectroscopy • nanoparticles

- [1] *Metal Nanoclusters in Catalysis and Materials Science: The Issue of Size Control*; Corain, B., Schmid, G., Toshima, N. ed.; Elsevier, **2007**; Vol. 10.
- [2] *Nanoparticles: from theory to application*; Schmid, G. ed.; Wiley-VCH: Weinheim, Germany, **2004**.
- [3] *Metal nanoparticles: synthesis, characterization and applications*; Marcel Dekker: New York, **2002**.
- [4] R. Shenhar, T. B. Norsten, V. M. Rotello, *Adv. Mater.* **2005**, *17*, 657-669.
- [5] S. Pathak, M. T. Greci, R. C. Kwong, K. Mercado, G. K. S. Prakash, G. A. Olah, M. E. Thompson, *Chem. Mat.* **2000**, *12*, 1985-1989.
- [6] S. Klingelhofer, W. Heitz, A. Greiner, S. Oestreich, S. Forster, M. Antonietti, *J. Am. Chem. Soc.* **1997**, *119*, 10116-10120.
- [7] U. Schlotterbeck, C. Aymonier, R. Thomann, H. Hofmeister, M. Tromp, W. Richtering, S. Mecking, *Adv. Funct. Mater.* **2004**, *14*, 999-1004.
- [8] R. M. Ormerod, R. M. Lambert, H. Hoffmann, F. Zaera, L. P. Wang, D. W. Bennett, W. T. Tysoe, *J. Phys. Chem.* **1994**, *98*, 2134-2138.
- [9] S. Kobayashi, R. Akiyama, *Chem. Commun.* **2003**, 449-460.
- [10] B. M. L. Dooos, I. F. J. Vankelecom, P. A. Jacobs, *Adv. Synth. Catal.* **2006**, *348*, 1413-1446.
- [11] C. Moreno-Marrodan, P. Barbaro, M. Catalano, A. Taurino, *Dalton Trans.* **2012**, *41*, 12666-12669.
- [12] L. S. Ott, R. G. Finke, *Coord. Chem. Rev.* **2007**, *251*, 1075-1100.
- [13] R. Akiyama, S. Kobayashi, *J. Am. Chem. Soc.* **2003**, *125*, 3412-3413.
- [14] C. Pan, K. Pelzer, K. Philippot, B. Chaudret, F. Dassenoy, P. Lecante, M. J. Casanove, *J. Am. Chem. Soc.* **2001**, *123*, 7584-7593.
- [15] Y. Borodko, H. S. Lee, S. H. Joo, Y. Zhang, G. Somorjai, *J. Phys. Chem. C* **2010**, *114*, 1117-1126.
- [16] F. Novio, D. Monahan, Y. Coppel, G. Antorrena, P. Lecante, K. Philippot, B. Chaudret, *Chem. Eur. J.* **2014**, *20*, 1287-1297.
- [17] H. Song, R. M. Rioux, J. D. Hoefelmeyer, R. Komor, K. Niesz, M. Grass, P. Yang, G. A. Somorjai, *J. Am. Chem. Soc.* **2006**, *128*, 3027-3037.
- [18] N. Yan, J. G. Zhang, Y. Tong, S. Yao, C. Xiao, Z. Li, Y. Kou, *Chem. Commun.* **2009**, 4423-4425.
- [19] R. Herbois, S. Noël, B. Léger, L. Bai, A. Roucoux, E. Monflier, A. Ponchel, *Chem. Commun.* **2012**, *48*, 3451-3453.
- [20] N. Yan, Y. Yuan, P. J. Dyson, *Chem. Commun.* **2011**, *47*, 2529-2531.
- [21] N. T. S. Phan, M. Van Der Sluys, C. W. Jones, *Adv. Synth. Catal.* **2006**, *348*, 609-679.
- [22] E. Groppo, W. Liu, O. Zavorotynska, G. Agostini, G. Spoto, S. Bordiga, C. Lamberti, A. Zecchina, *Chem. Mater.* **2010**, *22*, 2297-2308.
- [23] E. Groppo, G. Agostini, E. Borfecchia, L. Wei, F. Giannici, G. Portale, A. Longo, C. Lamberti, *J. Phys. Chem. C* **2014**, *118*, 8406-8415.
- [24] R. Grigg, L. X. Zhang, S. Collard, P. Ellis, A. Keep, *J. Organomet. Chem.* **2004**, *689*, 170-173.
- [25] E. Groppo, M. J. Uddin, O. Zavorotynska, A. Damin, J. G. Vitillo, G. Spoto, A. Zecchina, *J. Phys. Chem. C* **2008**, *112*, 19493-19500.
- [26] M. P. McCurdie, L. A. Belfiore, *Polymer* **1999**, *40*, 2889-2902.
- [27] K. H. Wu, Y. R. Wang, W. H. Hwu, *Polym. Degrad. Stabil.* **2003**, *79*, 195-200.
- [28] A. J. Pardey, A. D. Rojas, J. E. Yanez, P. Betancourt, C. Scott, C. Chinea, C. Urbina, D. Moronta, C. Longo, *Polyhedron* **2005**, *24*, 511-519.
- [29] L. A. Belfiore, M. P. McCurdie, E. Ueda, *Macromolecules* **1993**, *26*, 6908-6917.
- [30] L. A. Belfiore, H. Graham, E. Ueda, *Macromolecules* **1992**, *25*, 2935-2939.
- [31] L. A. Belfiore, A. T. N. Pires, Y. H. Wang, H. Graham, E. Ueda, *Macromolecules* **1992**, *25*, 1411-1419.
- [32] E. Groppo, M. J. Uddin, S. Bordiga, A. Zecchina, C. Lamberti, *Angew. Chem.-Int. Edit.* **2008**, *47*, 9269-9273.
- [33] L. Soptrajanova, B. Soptrajanova, *Spectroscopy Letters: An International Journal for Rapid Communication* **1992**, *25*, 1141 - 1151.
- [34] T. A. Stephenson, G. Wilkinson, *J. Inorg. Nucl. Chem.* **1967**, *29*, 2122-2123.
- [35] D. D. Kragten, R. A. van Santen, M. K. Crawford, W. D. Provine, J. J. Lerou, *Inorg. Chem.* **1999**, *38*, 331-339.
- [36] K. Nakamoto, *Infrared and Raman Spectra of Inorganic and Coordination Compounds*; John Wiley & Sons, Ltd, **2006**.

-
- [37] E. Stoyanov, *J. Struct. Chem.* **2000**, *41*, 440-445.
- [38] B. Abecassis, F. Testard, Q. Y. Kong, B. Francois, O. Spalla, *Langmuir* **2010**, *26*, 13847-13854.
- [39] B. Abecassis, F. Testard, O. Spalla, P. Barboux, *Nano Lett.* **2007**, *7*, 1723-1727.
- [40] M. Harada, N. Tamura, M. Takenaka, *J. Phys. Chem. C* **2011**, *115*, 14081-14092.
- [41] M. Harada, E. Katagiri, *Langmuir* **2010**, *26*, 17896-17905.
- [42] M. Harada, Y. Inada, *Langmuir* **2009**, *25*, 6049-6061.
- [43] M. Harada, K. Saijo, N. Sakamoto, H. Einaga, *Colloid Surf. A-Physicochem. Eng. Asp.* **2009**, *345*, 41-50.
- [44] J. Polte, T. T. Ahner, F. Delissen, S. Sokolov, F. Emmerling, A. F. Thunemann, R. Kraehnert, *J. Am. Chem. Soc.* **2010**, *132*, 1296-1301.
- [45] D. Tessier, A. Rakai, F. Bozonverduraz, *J. Chem. Soc.-Faraday Trans.* **1992**, *88*, 741-749.
- [46] L. L. Sheu, Z. Karpinski, W.-M. H. Sachtler, *J. Phys. Chem.* **1989**, *93*, 4890-4894.
- [47] S. Bordiga, E. Groppo, G. Agostini, J. A. Van Bokhoven, C. Lamberti, *Chem. Rev.* **2013**, *113*, 1736-1850.
- [48] L. Mino, G. Agostini, E. Borfecchia, D. Gianolio, A. Piovano, E. Gallo, C. Lamberti, *J. Phys. D-Appl. Phys.* **2013**, *46*.
- [49] C. Garino, E. Borfecchia, R. Gobetto, J. A. van Bokhoven, C. Lamberti, *Coord. Chem. Rev.* **2014**, *277-278*, 130-186.
- [50] C. Lamberti, E. Borfecchia, J. A. van Bokhoven, M. Fernández García, *XAS spectroscopy: Related Techniques and Combination with other spectroscopic and scattering Methods*, in: XAS and XES; Theory and Applications; van Bokhoven, J. A.; Lamberti, C., Ed.; John Wiley & Sons, **2015**; Vol. 1.
- [51] A. Longo, G. Portale, W. Bras, F. Giannici, A. M. Ruggirello, V. Turco Liveri, *Langmuir* **2007**, *23*, 11482-11487.
- [52] S. Nikitenko, A. M. Beale, A. M. J. van der Eerden, S. D. M. Jacques, O. Leynaud, M. G. O'Brien, D. Detollenaere, R. Kaptein, B. M. Weckhuysen, W. Bras, *J. Synchrot. Radiat.* **2008**, *15*, 632-640.
- [53] B. Ravel, M. Newville, *J. Synchrot. Radiat.* **2005**, *12*, 537-541.
- [54] A. P. Hammersley, S. O. Svensson, M. Hanfland, A. N. Fitch, D. Häusermann, *High Pressure Research* **1996**, *14*, 235-248.
-
